Vibration Measurement and Flutter Suppression Using Patch-type EFPI Sensor System

Do-Hyung Kim*

Rotorcraft Department
Korea Aerospace Research Institute, Daejeon, Korea 305-333

Jae-Hung Han and In Lee***

Division of Aerospace Engineering
Korea Advanced Institute of Science and Technology
Daejoen, Korea 305-701

Abstract

An optical phase tracking technique for an extrinsic Fabry-Perot interferometer (EFPI) is proposed in order to overcome interferometric non-linearity. Basic idea is utilizing strain-rate information, which cannot be easily obtained from an EFPI sensor itself. The proposed phase tracking system consists of a patch-type EFPI sensor and a simple on-line phase tracking logic. The patch-type EFPI sensor comprises an EFPI and a piezoelectric patch. An EFPI sensor itself has non-linear behavior due to the interferometric characteristics, and a piezoelectric material has hysteresis. However, the composed patch-type EFPI sensor system overcomes the problems that can arise when they are used individually. The dynamic characteristics of the proposed phase tracking system were investigated, and then the patch-type EFPI sensor system was applied to the active suppression of flutter, dynamic aeroelastic instability, of a swept-back composite plate structure. The proposed system has effectively reduced the amplitude of the flutter mode, and increased flutter speed.

Key Word : extrinsic Fabry-Perot interferometer, PZT, patch, flutter, control

Introduction

The optical fiber sensor systems have been successfully applied to the various engineering fields. The distributed sensing and monitoring of structures using optical fiber sensor network receive increasing intention in the field of aircraft or spacecraft engineering, where the reliability of lightweight structures are the key particulars. Among several kinds of optical fiber sensors, interferometric sensors are widely used because they have many advantages of general optical sensors and can be constructed at reasonable prices. However, it is reported that they have a problem of representing vibrational amplitudes and directions accurately because of their interferometric characteristics. In order to extract true mechanical strain from the EFPI output signal, several methods have been proposed including quadrature phase-shifted EFPI [1], absolute EFPI (AEFPI) [2], and passive quadratic signal processing using two read-out interferometers [3]. Several signal processing techniques have also been used based on fringe counting method [4, 5]. Such algorithms can be applicable to the strain measurement of quasi-static system, but are not

---

* Senior Research Engineer, Rotorcraft Department, KARI,
E-mail: dhkim@kari.re.kr,   Tel: 042-860-2286,   Fax: 042-860-2604
** Assistant Professor, Division of Aerospace Engineering, KAIST
*** Professor, Division of Aerospace Engineering, KAIST

practical for the real-time feedback control systems. Therefore, studies on the vibration control using interferometric optical fiber sensors have been limited to small disturbance cases [6]. In the authors' previous work [7], we experimentally investigated vibration control performance when the EFPI sensor produces non-linear signals. We examined the effects of non-linearity of the sensor on the control stability and performance, and investigated any simple method applicable to the vibrations beyond the linear range. For this purpose, a neural controller was utilized and its performance was experimentally investigated. It was found that the neural-network controller could suppress the non-linear vibration to some extent. However, an adaptive control algorithm such as a neural-network is not a fundamental solution to a dynamic system with highly non-linear sensing characteristics. Therefore, this paper establishes more practical method to extract vibration information from the EFPI sensor signal.

The aerospace engineering is one of the principal application fields of optical fiber sensors. Active researches on the health monitoring of aircraft structures have been performed, but dynamic application of optical fiber sensors are not throughly explored. For lightweight and flexible flight structures, it is important to measure and suppress the flow-induced vibrations such as flutter caused by interactions between fluid and structures. In recent years, several active control strategies have been studied in order to favorably modify the behavior of aeroelastic systems [8]. Active flutter suppression techniques can delay the onset of the flutter and enhance maneuver. The active flexible wing program has demonstrated the flutter suppression of a fighter-type scaled model in various maneuver modes by utilizing control surfaces and active control technology at NASA Langley research center [9]. The Benchmark Active Control Technology (BACT) model has been used as an active control test bed for evaluating new and innovative control methodologies [10]. Recent development of smart materials and structures gives us another alternative for active flutter suppression. Lazarus *et al.* [11] successfully applied multi-input multi-output controls to suppress vibration and flutter of a plate-like lifting surface with surface-bonded piezoelectric actuators. Han *et al.* [12] performed numerical and experimental investigation on active flutter suppression of a swept-back cantilevered plate using modern robust control theory. Application of piezoelectric actuation to flutter control of a more realistic wing model was achieved under the Piezoelectric Aeroelastic Response Tailoring Investigation program at NASA Langley research center [13].

This paper proposes a simple phase tracking system of the extrinsic Fabry-Perot interferometer (EFPI) sensor in order to overcome the interferometric non-linearity of the EFPI and experimentally demonstrates the performance of the proposed algorithms. The proposed phase tracking system consists of a patch-type EFPI sensor and an on-line phase tracking logic. The patch-type EFPI sensor comprises an EFPI and a piezoceramic (lead-zirconate-titanate, PZT) patch. An EFPI sensor itself has non-linear behavior due to the interferometric characteristics, and a PZT has hysteresis. However, the composed patch-type EFPI sensor system overcomes the problems that may arise when they used individually. Moreover, the proposed system can extract vibration information from the EFPI sensor signal with high non-linearity. In the first place, the dynamic characteristics of the proposed phase tracking system were investigated, and then the proposed sensor system was applied to a practical situation: aeroelastic control of a plate structure.

Patch-type EFPI sensor system

On-line phase tracking method

The operating mechanism of an EFPI sensor can be found in reference [7]. Its schematic diagram is shown in Fig. 1, where the reflected optical intensity, I, can be written as a sinusoidal function as follows:

$$I = A + B \cos \phi \tag{1}$$

where A and B are functions of the fiber core radius, the air gap separation, the transmission coefficient of the air/glass interface, and the numerical aperture; and ϕ is the optical phase. If the parameters A and B are assumed to be constant, the optical phase, ϕ, can be obtained as follows:

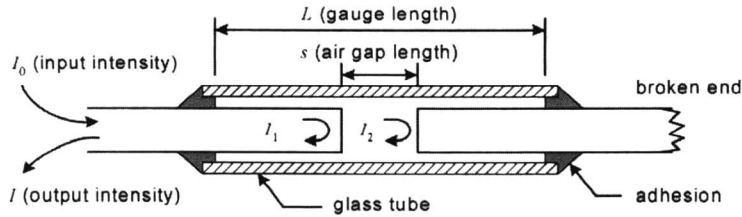$$\phi = \cos^{-1}\left(\frac{I-A}{B}\right) \tag{2}$$

Fig. 1. Schemetic diagram of EFPI.

When equation (2) is used for estimating mechanical strain from an EFPI sensor output signal, arc cosine function, however, has finite range between 0 and π. Accordingly, there exist discontinuous points. Because of this kind of discontinuity, direct evaluation of dynamic strain is not possible. Therefore, information about the direction of structural strain is necessary to solve the discontinuity problem. This directional information can be obtained from any other sensors that can produce real strain-rate. Among several kinds of sensors, piezoelectric material is used, in this paper. The patch-type EFPI sensor system considered in this study is the simple combination of existing two sensors: an EFPI and a PZT. By using the EFPI sensor signal and strain directional information, the optical phase, which corresponds to the mechanical strain, can be obtained as follows:

$$\phi_n = \phi_{n-1} + sign(\dot{\varepsilon}) \times \left| \cos^{-1}\left(\frac{I_n - A}{B}\right) - \cos^{-1}\left(\frac{I_{n-1} - A}{B}\right) \right| \tag{3}$$

where $\phi_n (=2ks)$ is the optical phase at n-th sampling step. The air cavity length, s, can be calculated using the optical phase, and then the strain can be obtained from the air cavity length. A high-pass filtering should be applied to remove any possible error that can arise from the phase accumulation.

Construction of sensor system

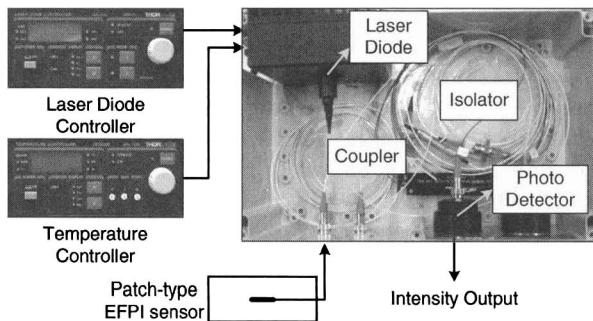The patch-type EFPI sensor system is proposed for the phase tracking method. An EFPI
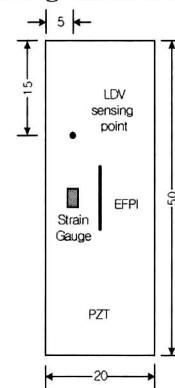

Fig. 2. EFPI sensor system

Fig. 3. Sensor placement

sensor is attached on a PZT, which produces strain-rate information. The patch-type EFPI sensor system consists of a PZT, an EFPI sensor, and an EFPI sensor system, which has a 1310 nm laser diode, an isolator, a photo detector, a 2 by 1 coupler, a laser diode controller, and a temperature controller. The overall configuration is shown in Fig. 2.

To begin with, the PZT output is observed in order to check the hysteretic behavior. The on-line phase tracking experiment has been performed using a composite plate model. The details of the test model will be described in the next section. The base PZT patch has 20 mm width and 50 mm length, and the fabricated EFPI sensor is bonded on the center of the PZT. An electric strain gauge and a Laser-Doppler Vibrometer (LDV: QFV303/3001, Polytec) are used for the comparison purpose. The location of each sensor is shown in Fig. 3. The plate is excited with its natural frequency, and the mechanical strain is recovered in real-time using the present phase tracking method, using a digital signal processing (DSP) board (DS1103, dSPACE).

To begin with, the PZT output is observed in order to check the hysteretic behavior. The relation of measured PZT output to displacement are shown in Fig. 4. The hysteretic behavior is observed from this figure. In addition, the PZT output grows to be saturated, according as the excitation amplitude increases. The hysteretic behavior itself is not worth considering in the phase tracking, because we just need the information of the sign of strain-rate. Hence, the PZT can be used in the phase tracking if the directional information can be extracted from the output. Simply, the differentiation of the PZT signal can be tried as shown in Fig. 5. In this case, we have to check whether the differential output corresponds to the strain-rate. Ideally, it is expected that all data points are located in the first or third quadrant. And the PZT output must be carefully scaled, because the saturation of PZT output and consequent error in strain-rate can raise a serious problem in phase tracking. If we use appropriately scaled PZT output without saturation, the hysteretic effects on strain-rate can be considered to be slight and the differential PZT signal can be used as directional information signal.
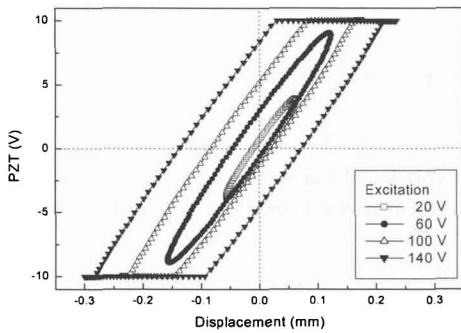

Fig. 4. Relation between PZT signal and displacement
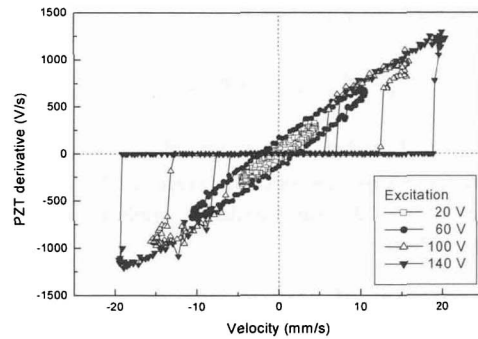

Fig. 5. Relation between derivative of PZT and velocity

Another alternative to differentiation is using a signal conditioning circuit. Within its linear region, PZT generates an electric charge proportional to the strain and the area of the PZT. Accordingly, the PZT can be considered to be charge generator. An electric circuit using operational amplifier with theoretically zero input impedance can be used as a signal conditioner [14]. The signal conditioner incorporated with the PZT is shown in Fig. 6. The output current of the PZT is simply the time derivative of the charge generated by the PZT. The output voltage of the signal conditioner is the negative of the product of the current and the feedback resistance R_f as follows:

$$V(t) = -R_f i(t) = -R_f \frac{dq(t)}{dt} \propto -R_f \dot{\varepsilon}(t) \tag{4}$$

Consequently, the output voltage in equation (4) is proportional to the strain-rate. The
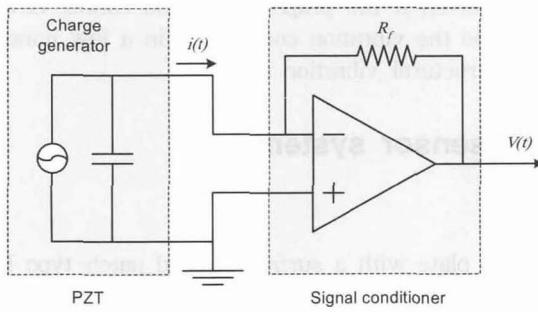
Fig. 6. PZT and signal conditioner
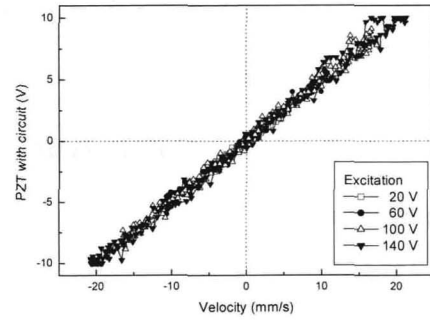
Fig. 7. Relation between circuit output and velocity

phase tracking method described in equation (3) uses only the sign of the strain-rate. Hence, the saturation is out of the question; which can be a problem in direct differentiation approach. The signal conditioner is also tested in vibration experiment. Fig. 7 is the relation of the circuit output to the velocity signal acquired by the LDV. In this case, almost all data points are located in the first and third quadrants. Therefore, the circuit output signal is regarded as strain-rate signal, accordingly the signal conditioning circuit can be effectively used for the proposed phase tracking method.

At this point, the construction of other types of patch-type EFPI sensor can be considered. The key point of patch-type EFPI sensor is the combination of EFPI and another sensor material which can produce directional information. The strain gauge, which is one of the most widely used and easily obtainable sensor, can be a candidate for a part of a patch-type EFPI sensor. However, the use of strain gauge for a patch-type EFPI sensor is not so useful. Because the strain gauge is not free from electric noise, there can be a serious problem in producing strain-rate information. The relation of circuit output and velocity is almost linear as shown in Fig. 7, however the relation between the circuit output and the derivative of strain gauge signal is not clear. The derivative of noisy strain gauge signal can produce much more noise as shown in Fig. 8. Therefore, the construction of current type sensor comprising PZT and EFPI is more practical and useful.
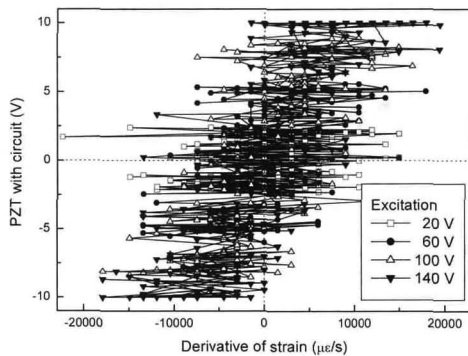
Fig. 8. Relation between circuit output and derivative of strain gauge
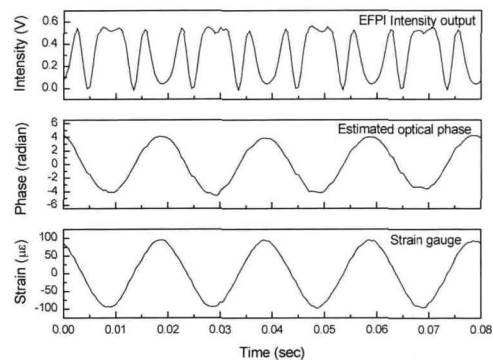
Fig. 9. Experimental result of phase tracking

Using proposed phase tracking method and the patch-type EFPI sensor system, the on-line phase tracking test has been performed. Fig. 9 shows an example of real-time phase tracking. The optical phase can be reconstructed from highly non-linear EFPI output signal, which cannot be easily obtained in real-time using conventional interferometric optical fiber sensors and signal processing techniques. The proposed patch-type EFPI sensor system is free from the hysteresis

of the PZT and the interferometric non-linearity. Even if the proposed method cannot cover a broad dynamic range, it can be practically applied to the vibration control within a few hundreds hertz, which it is interesting frequency range in structural vibration control.

Patch-type EFPI sensor system

System description

The test model is a swept-back cantilevered plate with a surface bonded patch-type EFPI sensor and piezoceramic actuators. The base plate is $[90_2/0_2]_s$ graphite/epoxy laminate (CU-125 NS, Hankuk Fiber). Four piezoceramic (C-82, Fuji Ceramics) actuators are bonded on the surface close to leading edge and one patch-type EFPI sensor (L= 6 mm, s = 14 μm) is bonded on the surface close to trailing edge as shown in Fig. 10.

Wind tunnel test has been performed in the subsonic wind tunnel at the Department of Aerospace Engineering, KAIST. The wind tunnel is an open-circuit tunnel with effective speed ranges of 9 to 60 m/sec and it has closed test section. In order to measure the vibration of the test model, a patch-type EFPI sensor, an electric strain gauge and a laser displacement sensor (LB301, KEYENCE) are used. The location of each sensor is described in Fig. 3. The experimental setup for the flutter suppression is shown in Fig. 11. A DSP board (DS1103, dSPACE) is used for the data acquisition and controller implementation. The generated control input is applied to the piezoceramic actuators through a high voltage amplifier (PSZ 700-2, TREK).

Fig. 10. Wind tunnel test model

Fig. 11. Experimental setup for flutter suppression

Flutter analysis and open loop wind tunnel experiment

At first, modal testing was performed and compared with the result of the MSC/NASTRAN. The material properties of CU-125 NS is as follows:

$$E_1 = 119\ GPa, E_2 = 8.67\ GPa, G_{12} = G_{13} = 5.18\ GPa,$$
$$G_{23} = 3.29\ GPa, \nu_{12} = 0.31, \rho = 1570\ kg/m^3, t = 0.1225\ mm \tag{5}$$

The structural effects of PZT and optical fiber were assumed to be negligible, so the base plate is only considered in the analysis. Six by twelve QUAD4 2-D Shell elements are used for

normal mode analysis. The experimental and analytic modal frequencies are shown in Table 1. The experimental modal frequencies are close to analytic results.

Table 1. Modal frequencies of the test model.

Mode No.	Modal frequency (Hz)		
	Experiment (plate w/ front PZTs)	Experiment (plate w/ all PZTs)	MSC/NASTRAN
1	11.91	12.16	11.93
2	48.64	49.14	48.46
3	84.31	84.86	83.03
4	120.16	119.77	128.16

The aeroelastic analysis can be subdivided into two methods. One is frequency domain analysis: V-g method. The other is time domain analysis: the time integration of aeroelastic equation. Frequency domain and time domain methods have different approaches, but these methods give similar solution for linear aeroelastic problems [15]. Because the frequency domain analysis has the advantages of relatively less computation time, simple analysis procedure, and ease of physical interpretation, the V-g method is applied and the MSC/NASTRAN [16] is used for linear aeroelastic analysis. The V-g plot is shown in Fig. 12. It can be seen that the second mode becomes unstable as the airflow speed increases, and the flutter speed is $V_F = 33.5$ m/s. Another particular characteristic for an aeroelastic system is frequency changes according to airflow speed, which is shown in Fig. 13, V-f plot.
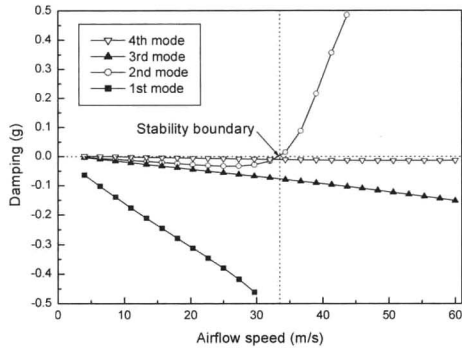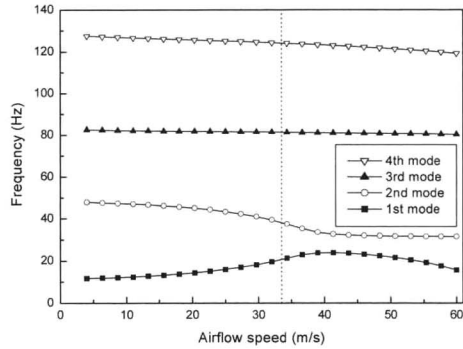

Fig. 12. V-g plot of the test model

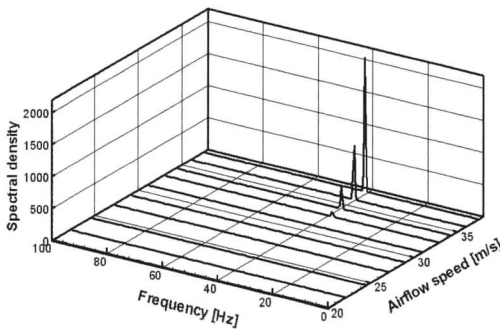**Fig. 13. V-f plot of the test model**

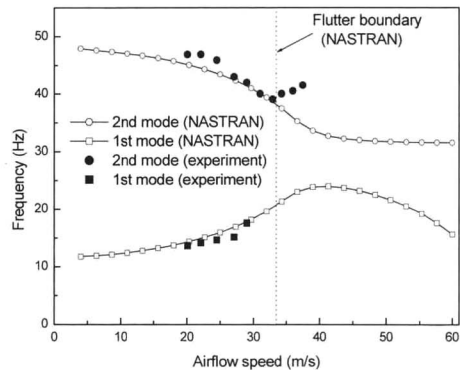**Fig. 14. Power spectra vs. airflow speed frequencies**

Fig. 15. The first and the second modal of the test model

When the test model is exposed to the aerodynamic loading in the wind tunnel, air damping is dominant and the aeroelastic system is stable in case that the airflow speed is below 30 m/s. As the airflow speed increases, the limit cycle oscillation occurs and the vibration amplitude increases according to the airflow speed. Power spectra of the strain against airflow speed are shown in Fig. 14. It can be found that the vibration energy is concentrated in the flutter mode and increases according to the airflow speed.

A change of the dynamic characteristics appears when the airflow speed is around 33 m/s. In case where the airflow speed is over 33 m/s, the limit cycle oscillation starts to be observed with the naked eye. Therefore, it can be inferred that the flutter boundary exists around the air speed of 33 m/s. Another phenomenon that we can observe is the changes of modal frequencies. The first and the second modal frequencies are compared with analytic results in Fig. 15. The experimental modal frequencies are close to analytic results when the airflow speed is below flutter boundary. As the airflow speed increases, the vibration energy is concentrated on the second mode. Therefore, identification of other modes is difficult except the second mode. And a noticeable phenomenon is that the changing direction of the second modal frequency is opposite to the analytic result. The flutter is a non-linear phenomenon, however, the V–g analysis is a linear tool. Therefore, the analytic result does not guarantee the reliable result for the post-flutter phenomenon. The point where the second modal frequency takes the opposite changing direction can be another clue to the flutter boundary. The boundary of this discrepancy is 33 m/s. It is consistent with the airflow speed where large amplitude limit cycle oscillation arises.

Flutter suppression experiment

Since the aeroelastic phenomena are the result of the interactions between fluid and structures, dynamic characteristics of an aeroelastic system change according to the airflow speed. Therefore, it is difficult to obtain exact numerical model, and the adaptiveness and robustness are important features for an aeroelastic control system. Hence, adaptive or robust controller is preferred for the control of aeroelastic system. In the present study, major matter of concern is the investigation of the capacity of the proposed patch-type EFPI sensor system. So, a simple control algorithm is firstly applied. If we know the vibrational frequency, a positive position feedback (PPF) controller can be a candidate for the vibration suppression system. The frequency of the second mode of the test model at the airflow speed around flutter boundary is about 40 Hz. Although second modal frequency in the still air is 48.6 Hz and it decreases to 40 Hz at U = 33 m/s, it is assumed that the sensor and actuator has the same phase difference as in the still air. And the damping parameter of the PPF controller is set to be 0.3 for the purpose of maintaining robustness to frequency variations. The designed PPF controller is as follows:
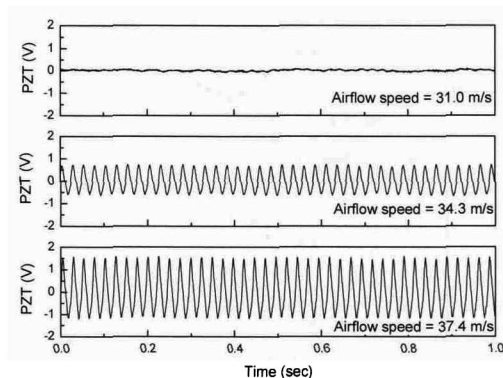

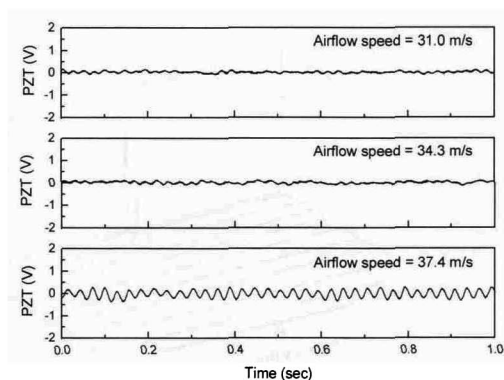Fig. 16. **Uncontrolled time history of the PZT signal**

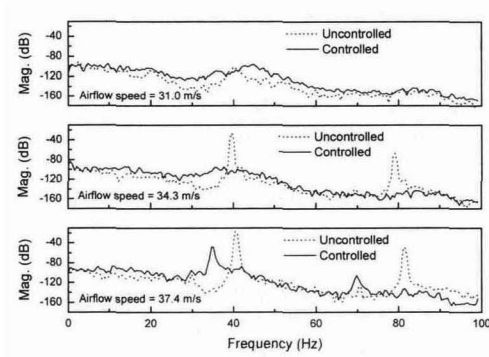Fig. 17. **Controlled time history of the PZT signal**
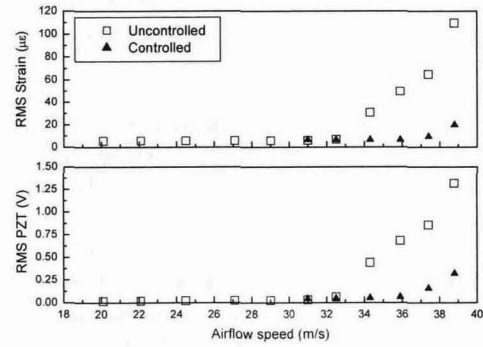
Fig. 18. Power spectra of the PZT signal   Fig. 19. RMS value of strain and PZT signal

$$H(s) = \frac{\omega_f^2}{s^2 + 2\zeta\omega_f s + \omega_f^2}$$
$$\omega_f = 2\pi \times 40 \,(rad/\sec), \ \zeta = 0.3 \tag{6}$$

Control result in time domain is shown in Fig. 16 and 17, and power spectra at several airflow speeds is shown in Fig. 18. Finally, the RMS values are represented in Fig. 19. The PPF controller shows excellent performance as a whole. It can be found that the airflow speed where the RMS values begin to increase is delayed about 4 m/s. Accordingly, the flutter boundary is increased over 10 % by applying the PPF controller.

Conclusions

In the present study, the development of patch-type EFPI sensor system and its application to flutter suppression have been investigated. An on-line phase tracking method was proposed for the purpose of extracting dynamic mechanical strain information from non-linear sensor signal in real-time. The proposed method can be practically applied to the vibration control within a few hundreds hertz frequency. A patch-type EFPI sensor system was constructed and applied to flutter suppression. The proposed patch-type EFPI sensor system is free from the interferometric non-linearity of EFPI sensor and hysteresis of PZT. By applying a PPF controller, an increase of 10 % in flutter boundary is obtained. The stability boundary and reliability of an aeroelastic system could be increased by integrating smart materials into advanced structures.

Acknowledgement

References

1. Murphy, K. A., Gunther, M. F., Vengsarkar, A. M., and Claus, R. O., "Quadrature phase-shifted, extrinsic Fabry-Perot optical fiber sensors", *Optics Letters*, Vol. 16, No. 4, 1991, pp. 273-275.

2. Tran, T. A., Greene, J. A., Murphy, K. A., and Bhatia, V., "EFPI manufacturing improvements for enhanced performance and reliability", *Proc. of SPIE 2247*, 1995, pp. 312-323.

3. Lo, Y.-L. and Sirkis, J. S., "Passive Signal Processing of In-Line Fiber Etalon Sensors for High Strain-Rate Loading", *Journal of Lightwave Technology*, Vol. 15, No. 8, 1997, pp. 1578-1586.

4. Kim, S.-H., Lee, J.-J., and Kwon, D.-S., "Signal processing algorithm for transmission-type Fabry-Perot interferometric optical fiber sensor", *Smart Materials and Structures*, Vol. 10, No. 4, 2001, pp. 736-742.

5. Kwon, I. B., Kim, C. G., and Hong, C. S., "A digital signal processing algorithm for structural strain measurement by 3x3 passive demodulated fiber optic interferometric sensor", *Smart Materials and Structures*, Vol. 8, No. 4, 1999, pp. 433-440.

6. Kim, D.-H., Han, J.-H., Yang, S.-M., Kim, D.-H., Lee, I., Kim, C.-G. and Hong, C.-S., "Optimal Vibration Control of a Plate Using Optical Fiber Sensor and PZT Actuator", *Smart Materials and Structures*, Vol. 12, No. 4, 2003, pp. 507-513.

7. Kim, D.-H., Han, J.-H., Kim, D.-H., Lee, I., "Vibration control of structures with interferometric sensor non-linearity", *Smart Materials and Structures*, Vol. 13, No. 1, 2004, pp. 92-99.

8. Dowell, E. H., Crawley, E. F., Curtiss Jr., H. C., Peters, D. A., Scanlan, R. H., and Sisto F., A Modern Course in Aeroelasticity, 3rd Ed., Kluwer Academic Publishers, Dordrecht, 1995.

9. Waszak, M. R. and Srinathkumar, S., "Flutter Suppression for the Active Flexible Wing: A Classical Approach", *Journal of Aircraft*, Vol. 32, No. 1, 1995, pp. 61-67.

10. Waszak, M. R., 1998, "Modeling the Benchmark Active Control Technology Wind-Tunnel Model for Active Control Design Application", NASA TP-1998-206270, June 1998.

11. Lazarus, K. B., Crawley, E. F. and Lin, C. Y., "Multivariable Active Lifting Surface Control Using Strain Actuation: Analytical and Experimental Results", *Journal of Aircraft*, Vol. 34, No. 3, 1997, pp. 313-321.

12. Han, J.-H., Tani, J. and Lee, I., "Flutter Suppression of a Lifting Surface Using Piezoelectric Actuation", *Proceedings of The Second Asian-Australasian Conference on Composite Materials*, Kyongju, Korea, 2000, pp. 843-848.

13. Heeg, J., "Analytical and Experimental Investigation of Flutter Suppression by Piezoelectric Actuation", NASA TP-3241, February 1993.

14. Sumali, H., Meissner, K., and Cudney, H. H., "A piezoelectric array for sensing vibration modal coordinates", *Sensors and Actuators A*, Vol. 93, No. 2, 2001, pp. 123-131.

15. Bae, J.-S., Yang, S.-M., and Lee, I., "Linear and Nonlinear Aeroelastic Analysis of Fighter-Type Wing with Control Surface", *Journal of Aircraft*, Vol. 39, No. 4, 2002, pp. 697-708.

16. Rodden, W. P., and Johnson, E. H., MSC/NASTRAN Version 68 Aeroelastic Analysis User's Guide, MacNeal-Schwendler, Los Angeles, 1994.